ChemPubSoc Europe

DOI: 10.1002/cssc.201700589

CHEMSUSCHEM Full Papers

# Gliding Arc Plasmatron: Providing an Alternative Method for Carbon Dioxide Conversion

Marleen Ramakers,* Georgi Trenchev, Stijn Heijkers, Weizong Wang, and Annemie Bogaerts*[a]

Low-temperature plasmas are gaining a lot of interest for environmental and energy applications. A large research field in these applications is the conversion of $CO_2$ into chemicals and fuels. Since $CO_2$ is a very stable molecule, a key performance indicator for the research on plasma-based $CO_2$ conversion is the energy efficiency. Until now, the energy efficiency in atmospheric plasma reactors is quite low, and therefore we employ here a novel type of plasma reactor, the gliding arc plasmatron (GAP). This paper provides a detailed experimental and computational study of the $CO_2$ conversion, as well as the energy cost and efficiency in a GAP. A comparison with thermal conversion, other plasma types and other novel $CO_2$ conversion technologies is made to find out whether this novel plasma reactor can provide a significant contribution to the much-needed efficient conversion of $CO_2$. From these comparisons it becomes evident that our results are less than a factor of two away from being cost competitive and already outperform several other new technologies. Furthermore, we indicate how the performance of the GAP can still be improved by further exploiting its non-equilibrium character. Hence, it is clear that the GAP is very promising for $CO_2$ conversion.

## Introduction

Global warming owing to the increasing emissions of greenhouse gases is a hot topic nowadays.[1] Burning fossil fuels has led to the emission of large amounts of $CO_2$, which contributes to 70% to the overall global warming. Since the industrial revolution, the atmospheric $CO_2$ concentration has been increasing from 278 to 407 ppm as reported in March 2017.[2] This rise is owed to the fact that anthropogenic $CO_2$ emissions outpace the natural carbon cycle. Therefore, the conversion of this main greenhouse gas into value-added products, like feedstock for the chemical industry or liquid fuels, is considered as the challenge of this century.[3,4] The current conversion methodologies not only aim to tackle climate change, but also to provide a solution for our dependence on fossil fuels if renewable energy sources are being used. Turning a waste product like $CO_2$ into new feedstock fits in the framework of green chemistry and also complies with the "cradle-to-cradle" principle.[5] In this way, the carbon loop can be closed.

The urgent need for $CO_2$ conversion results in a booming interest for various conversion technologies, such as photochemical, electrochemical and thermochemical pathways, either with or without catalysts, and all their possible combinations.[6–12] Another conversion technology that is intensively investigated is the use of plasma.[13] Plasma is created by applying electric power to a gas, causing breakdown of the gas into ions and electrons. It is thus a (partially) ionized gas, consisting of molecules, but also a large number of other species, such as various radicals, ions, excited species, and electrons. This makes plasma a highly reactive cocktail, useful for many applications.[14] The main advantage of plasma is that mainly the electrons are heated by the applied power, because of their small mass, and the energetic electrons can activate the gas by electron impact excitation, ionization, and dissociation, creating reactive species that can easily form new molecules. In this way, the gas as a whole does not have to be heated. Furthermore, owing to the fact that plasma can be switched on and off very easily, this technique could also have great potential to store intermittent renewable energy, like solar and wind.

Due to its increasing interest, many researchers are investigating the splitting of $CO_2$ into CO and $O_2$ by plasma,[15–37] both in pure $CO_2$ as well as in a mixture with other gases like $CH_4$,[38–55] $H_2$,[40,56,57] or $H_2O$.[40,58–60] When $CO_2$ is mixed with such a hydrogen source, value-added chemicals can be produced, such as syngas, methanol, formaldehyde and formic acid. Most research on plasma-based $CO_2$ conversion is done with one of the following types of plasmas: dielectric barrier discharges (DBD),[15–21,36–47,49–52,61,62] microwave (MW) plasmas,[21–25,30–33,38–40,54,59] nanosecond-pulsed plasmas (NSP),[35,63] spark discharges,[64–66] and gliding arc discharges.[26–28,38,39,55,67] A lot of research goes into improving the energy efficiency of the process. In this respect, gliding arc plasmas are among the most promising, because they typically produce electrons with energy around 1 eV. This energy is ideal for vibrational excita-

[a] M. Ramakers, G. Trenchev, S. Heijkers, Dr. W. Wang, Prof. Dr. A. Bogaerts
Department of Chemistry, Research group PLASMANT
University of Antwerp
Universiteitsplein 1, 2610 Wilrijk (Belgium)
E-mail: marleen.ramakers@uantwerpen.be
annemie.bogaerts@uantwerpen.be

The Supporting Information and ORCID identification number(s) for the author(s) of this article can be found under https://doi.org/10.1002/cssc.201700589.

tion of $CO_2$, which is seen as the most efficient way to split this molecule.[21]

Although the gliding arc discharge seems a good match for $CO_2$ conversion, only limited studies have been performed. Moreover, most of these studies are performed with classical gliding arc reactors. The latter configuration, however, has a few disadvantages. Indeed, it is incompatible with various industrial systems because of its 2D geometry, the gas treatment is non-uniform because only a limited fraction of the gas passes through the arc, and the residence time inside the plasma is quite short. To overcome these drawbacks, a 3D gliding arc reactor with specific gas-flow configuration, also called gliding arc plasmatron (GAP), was recently developed.[28] This reactor design is very promising because it can be implemented in industry and the specific gas flow configuration ensures the gas treatment to be uniform, while it forces a longer residence time inside the arc plasma. Despite these advantages, only one paper for $CO_2$ conversion with such a reactor is published to our knowledge,[28] and there is clearly more research needed to fully exploit the capabilities of this new type of plasma reactor.

Therefore, here, we perform a detailed, combined experimental and computational study, to explore the possibilities of the GAP for $CO_2$ conversion. We study in detail the effect of the flow configuration, that is, vortex flow, as well as the effect of the flow rate and the plasma power, on the $CO_2$ conversion and corresponding energy cost and energy efficiency of the process. By comparing these values with those for pure thermal conversion, we can clearly demonstrate the non-equilibrium character of the conversion process, in which the gas as a whole does not have to be heated, explaining the higher values of conversion and energy efficiency. Furthermore, the experiments are supported by chemical reaction simulations and by simulations of the gas flow and the arc plasma movement, to obtain in-depth knowledge on the underlying mechanisms. Finally—and most importantly from a possible future implementation point-of-view—we will benchmark our results with data obtained in other plasma reactors as well as with data obtained with other novel $CO_2$ conversion technologies, to provide a global overview of the capabilities of plasma technology for $CO_2$ conversion, and especially of the position of the GAP in this context.

## Results and Discussion

First, we will present and discuss the experimental results for different values of plasma power and flow rate. Next, we will illustrate the effect of the vortex flow for the three different configurations (i.e., anode diameters). These results will be compared with the theoretical thermal conversion and energy efficiency. Subsequently, we will compare the experimental results with model predictions, and we will use the model for a detailed analysis of the underlying plasma chemistry. Finally, we will benchmark our results with different plasma setups and make a comparison with other novel $CO_2$ conversion technologies.

### Effect of power and flow rate on $CO_2$ conversion, energy cost, and energy efficiency

The experiments were conducted for five different flow rates and eight different values of plasma power. We show here the results for the configuration with anode diameter of 14.20 mm. The results for the other configurations can be found in the Supporting Information.

Figure 1a shows the conversion plotted as a function of plasma power for the five different flow rates. The values are in the order of 1–6%. Below 225 W the arc is in a so-called low-current regime around 50 mA, whereas above 475 W a so-called high-current regime is obtained, with current values between 260 and 380 mA. In between these two regimes, no stable plasma could be formed with this power supply. If we compare these two regimes, it is obvious that the conversion is lower in the low-current regime than in the high-current regime. This can of course be explained by the lower current and plasma power. A lower current simply means fewer electrons, which can be used to split $CO_2$. In addition, also the power is lower, so less energy is available to convert $CO_2$. However, if the plasma power increases in its own regime, this has no significant effect on the $CO_2$ conversion. Instead, the extra energy available will be used to heat up the gas, as is shown in Figure 1d.

In contrast to the plasma power, the gas flow rate has a visible effect on the $CO_2$ conversion: the lower the flow rate, the higher the conversion, both in the low- and high-current regime. This is obviously owed to the longer residence time of the gas in the plasma. Further decreasing the flow rate to increase the conversion is, however, not possible in our setup, because a minimum flow rate is necessary to obtain a good vortex flow. Furthermore, the increase in conversion facilitated by lowering the flow rate overall results in less $CO_2$ converted, in liters per minute. This is less interesting from industrial point of view. The flow rate is thus limited, but the residence time, and therefore probably also the conversion, might be further increased by increasing the length of the cathode. This will be explored in more detail in our future work, as we need to be verify whether this still allows to create a good vortex flow pattern.

Figure 1b,c shows the energy cost and energy efficiency, respectively. It is clear that in some cases the energy cost is lower and the energy efficiency is higher in the low-current regime than in the high-current regime. However, the corresponding conversion in these cases is quite low (see Figure 1a), so these cases are overall not so interesting. In the high-current regime there is no significant change in the energy cost or in the energy efficiency when increasing the plasma power. In general, the energy cost is slightly lower and the energy efficiency is slightly higher for higher flow rates at constant plasma power. All these trends can be explained from Equations (4) and (5) in the Experimental Section. The values of energy cost and energy efficiency are in the range of 25–66 kJ $L^{-1}$ (or 6.3–16.4 eV $molec^{-1}$) and 18–46%, respectively, which are already quite good compared to other plasma technologies, as will be elaborated in more detail below.

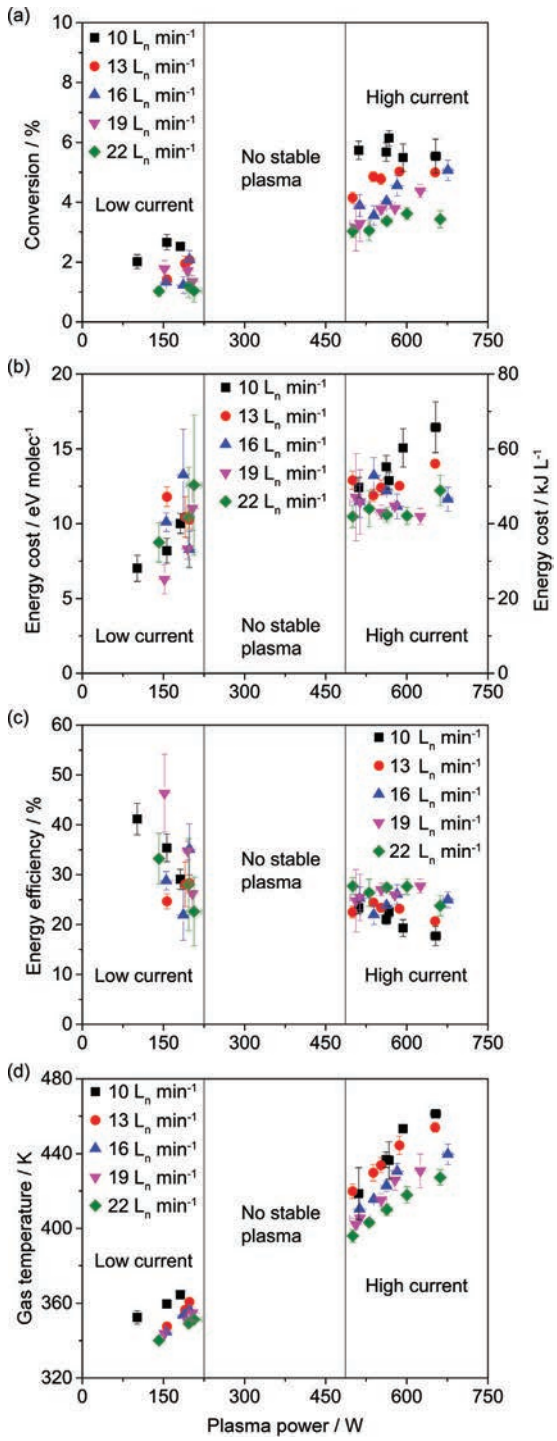


**Figure 1.** a) Conversion, b) energy cost, c) energy efficiency, d) and gas temperature of the effluent stream as a function of plasma power for five different flow rates, for the configuration with anode diameter of 14.20 mm.

We are not able to measure the gas temperature inside the arc, but we measured the temperature of the effluent stream (Figure 1 d), and it shows the same trends as the conversion. The temperature rises more or less linearly with the plasma power, which is logical because more energy is available to heat up the gas. Furthermore, at constant plasma power, the gas temperature is slightly higher at lower flow rate, because of the longer residence time of the gas in the plasma, giving more time to heat up the gas. The temperature values inside the plasma are of course much higher (see the Supporting Information), and the gas cools down significantly when leaving the reactor, but the temperature of the effluent stream can still reach values up to 450 K, which offers opportunities in the future to insert a catalyst in the reactor tube, for so-called plasma catalysis when mixing $CO_2$ with a suitable hydrogen source to realize more selective $CO_2$ conversion into targeted value-added chemicals.

In Figure 2, we combine all data of Figure 1 by plotting the results as a function of the specific energy input (SEI) for the five different flow rates investigated. The SEI is indeed a very

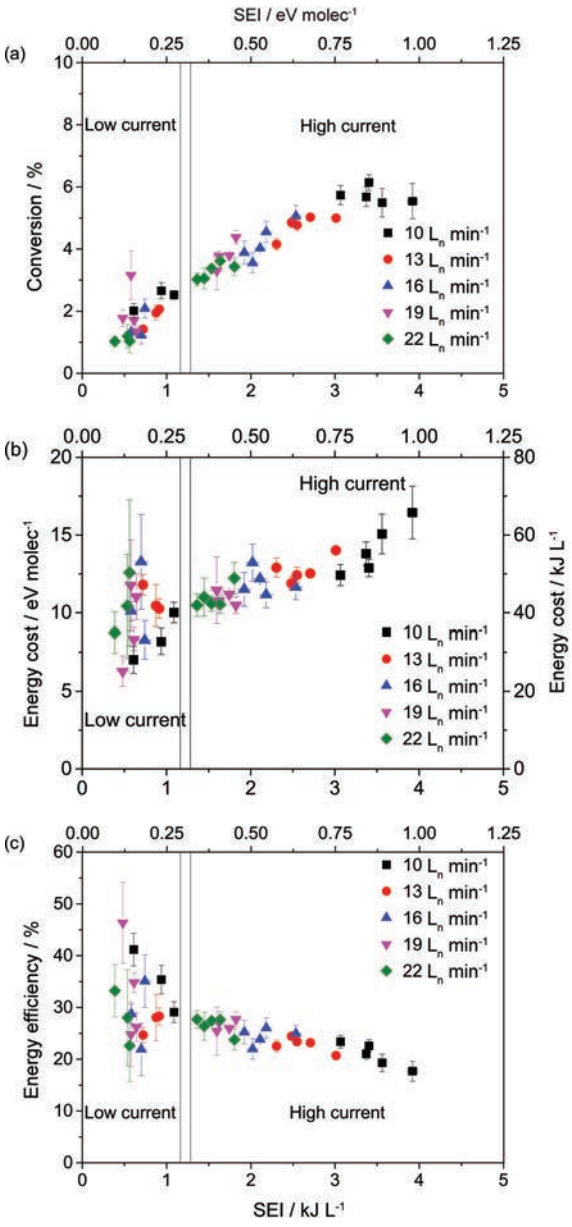


**Figure 2.** a) Conversion, b) energy cost, and c) and energy efficiency as a function of SEI for five different flow rates, for the configuration with anode diameter of 14.20 mm. The SEI is not only expressed in kJ $L^{-1}$, but also in eV $molec^{-1}$, which is commonly done in plasma research.

important parameter in plasma-based $CO_2$ conversion, as it combines the effect of power and gas flow rate [see Equation (3) in the Experimental Section]. The SEI values are depicted in the figure both in eV molec$^{-1}$, which is of interest from the point of view of the plasma chemistry, to explain the good energy efficiency (see below), as well as in kJ L$^{-1}$, which is of more practical interest for the applications. Again the low- and high-current regime can be distinguished. The conversion increases more or less linearly with rising SEI, which is logical as more energy per molecule is available to convert $CO_2$. Because the conversion rises slightly less than the rise in SEI (i.e., slope $\approx$0.7), the energy cost slightly rises, and the energy efficiency slightly decreases, as a function of the SEI, which can be explained from Equations (4) and (5) in the Experimental Section.

### Effect of the vortex flow on $CO_2$ conversion, energy cost, and energy efficiency

As further explained in the description of the experiments, the outlet of the reactor, which acts as the anode, is replaceable, and this will affect the vortex flow pattern. Hence, we want to investigate whether the latter will also affect the $CO_2$ conversion. For this comparison, diameters of 7.08, 14.20, and 17.50 mm are examined. Figure 3 shows the conversion (a), as well as energy cost (b), and energy efficiency (c) as a function of the SEI for the three studied configurations, for all combinations of gas flow rate and plasma power investigated. It is clear that the highest conversion (i.e., almost 9%) can be reached in the configuration with anode diameter of 7.08 mm and it decreases with increasing anode diameter. For each configuration, the conversion increases with rising SEI, as explained in the previous section.

For SEI values below 1 kJ L$^{-1}$ (low-current regime) results could only be obtained for the configuration with anode diameter of 14.20 mm. The reason is that the power supply could not sustain a stable discharge for the other configurations in this regime. It is clear from Figure 3 b,c that the energy cost in this case is slightly lower and the energy efficiency is slightly higher than the lowest/highest values, respectively, obtained with an anode diameter of 7.08 mm. However, the corresponding conversion is very low, making this regime overall not very suitable. Above 1.5 kJ L$^{-1}$ (high-current regime), the energy cost obtained in the configuration with anode diameter of 7.08 mm is again the lowest and the energy efficiency is again the highest. In general, the energy cost and efficiency stay more or less constant or slightly increase/decrease, respectively, with increasing SEI, depending on how much the conversion rises with SEI, as explained in the section above [see again Equations (4) and (5) in the Experimental Section]. Overall, we can conclude that the configuration with the smallest anode diameter gives the best performance for both the $CO_2$ conversion and energy cost/efficiency, reaching values of 8.6% conversion at an energy cost of 39 kJ L$^{-1}$ (or 9.7 eV molec$^{-1}$) and an energy efficiency of 30%. The best energy efficiency reached with this configuration is 35%, corresponding to an energy cost of 33 kJ L$^{-1}$ (or 8.3 eV molec$^{-1}$), but the conversion in this case is slightly lower, that is, 5.1%.

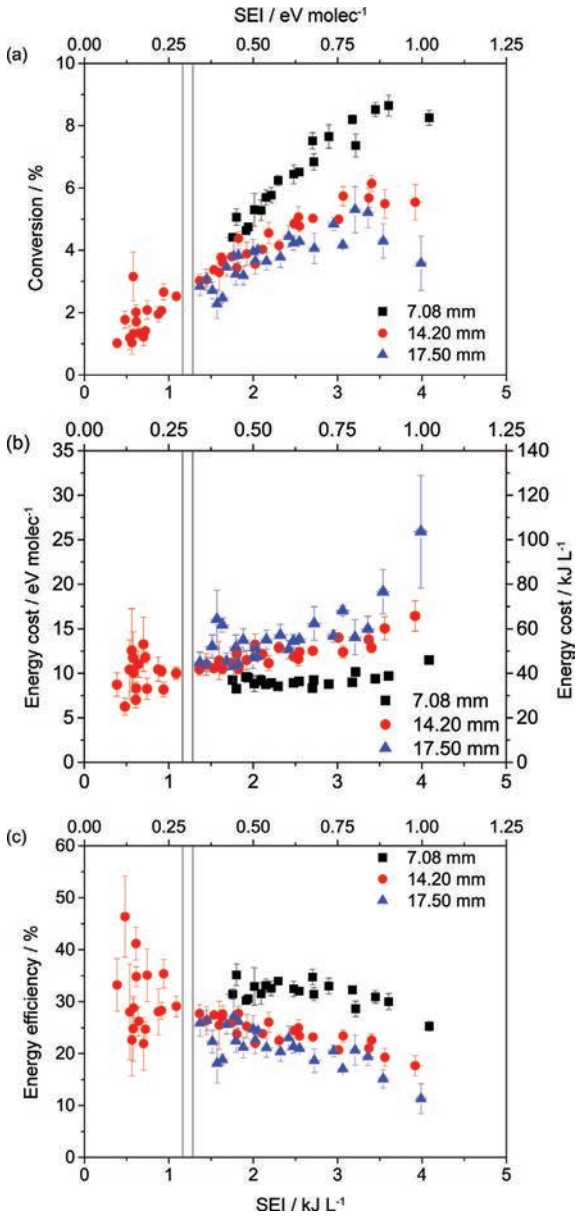


**Figure 3.** a) Conversion, b) energy cost, and c) energy efficiency as a function of the SEI for the three studied configurations, with three different anode diameters, as indicated by the legend.

The reason why the configuration with the smallest diameter gives the best results is that the reverse vortex flow (RVF) is most strongly pronounced, whereas in the configuration with the largest diameter, the RVF is almost non-existent. This is further elaborated in detail in the Supporting Information, based on gas-flow calculations for the different setups. The RVF forces a higher residence time of the gas in the reactor, and thus, in the arc discharge. Also, it provides thermal insulation of the discharge from the side walls, as the mass transfer always takes place from the walls to the plasma. This improves the ionization, excitation, and dissociation efficiency in the plasma, as it lowers the thermal losses due to cooling by the walls.

### Comparison of our results with thermal conversion and energy efficiency

To evaluate the performance of the GAP for $CO_2$ conversion, we compare our results with the calculated theoretical conversion and energy efficiency for a temperature range of 300–5000 K, in case of pure thermal $CO_2$ conversion. A detailed description of the calculation of this conversion and energy efficiency as well as of the SEI values in this case can be found in the Supporting Information.

The thermal conversion and corresponding energy efficiency are plotted as a function of the applied SEI in Figure 4. The $CO_2$ conversion and energy efficiency obtained in our GAP for the configuration with anode diameter of 7.08 mm are also plotted for comparison. It is obvious that the SEI applied to the GAP is typically below 4 kJ $L^{-1}$ or 1 eV $molec^{-1}$ (see also Figures 2 and 3 ), but in Figure 4 we show the results for the thermal calculations up to much higher SEI values, just to illustrate that the thermal conversion and energy efficiency at the typical SEI values as used in our GAP are virtually negligible, and only evolve to higher values above 4 kJ $L^{-1}$ (or 1 eV $molec^{-1}$).

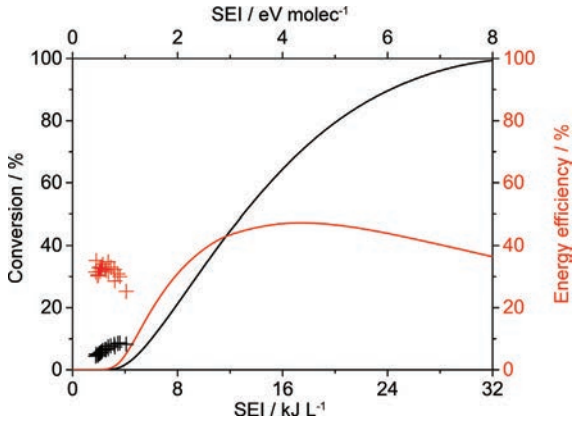


**Figure 4.** Calculated theoretical thermal conversion (left *y*-axis) and corresponding energy efficiency (right *y*-axis) as a function of specific energy input for pure $CO_2$ at a pressure of 1 atm, and comparison to our results (crosses) obtained in the GAP for the configuration with anode diameter of 7.08 mm.

To summarize, Figure 4 clearly demonstrates that both the conversion and especially the energy efficiency of $CO_2$ splitting in the GAP are much higher than for pure thermal conversion, in which the values are still negligible in the range of SEI values applied to the GAP. This better performance of the GAP can be explained by the non-equilibrium properties of the gliding arc plasma, as the electrons have a higher temperature than the gas (i.e., ca. 1.68 eV or 19500 K vs. up to 3000 K for the gas; see the section on plasma chemistry simulations in the Supporting Information), and these highly energetic electrons induce different chemical reactions. These chemical reactions will be further elaborated in the next section.

### Comparison of our results with model calculations and explanation of the underlying mechanisms

Figure 5 illustrates the calculated conversion (a), energy cost (b), and energy efficiency (c), as a function of SEI, for the GAP configuration with anode diameter of 7.08 mm, in comparison with the experimental data. The same rising trend is observed for the conversion, whereas the energy cost and efficiency do not vary a lot within the entire range of SEI values, similar to the experimental data. Moreover, also the absolute values are in excellent agreement, certainly when taking into account the complexity of the plasma chemistry and the assumptions in-

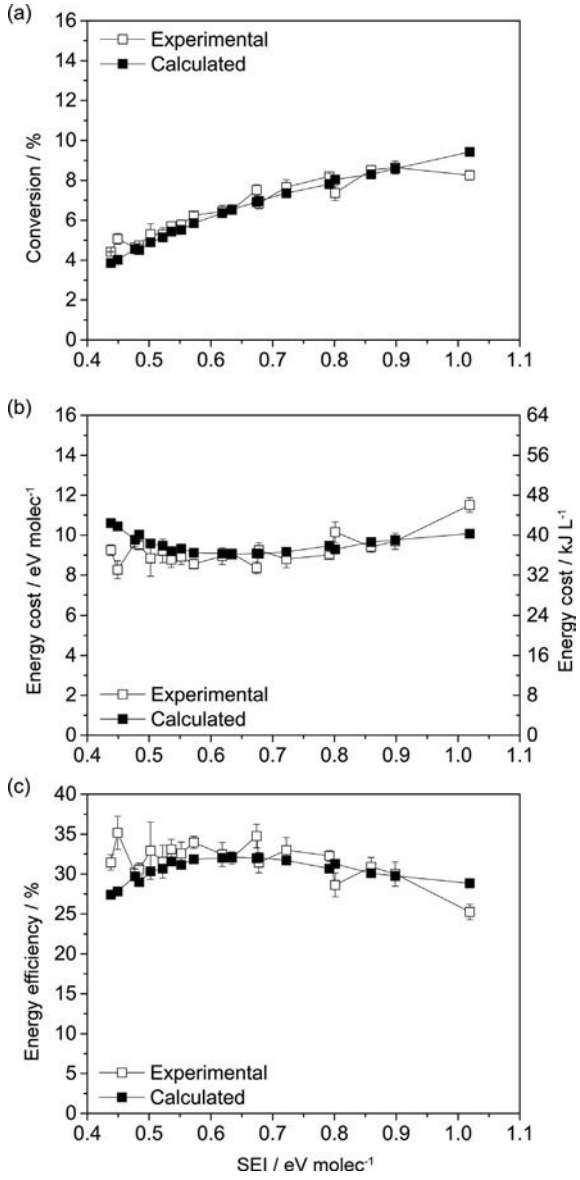


**Figure 5.** Calculated (full symbols) and measured (open symbols) a) conversion, b) energy cost, and c) energy efficiency as a function of SEI, for the configuration with anode diameter of 7.08 mm. Note that some discontinuities are observed in the data as a function of SEI. The reason is that the SEI is composed of plasma power and gas flow rate, and different combinations of plasma power and gas flow rate can give rise to the same SEI, but can also yield slightly different conversion, energy cost, and energy efficiency.

herent to a 0D model. This good agreement, in addition to the realistic values calculated by this model for the gas temperature, electron density, and temperature (see details in the Supporting Information), indicates that the model provides a realistic picture of the plasma chemistry in the GAP, and can thus be used to investigate the underlying mechanisms of the $CO_2$ conversion.

In Figure 6, we plot the relative contributions of the various $CO_2$ dissociation processes to the overall $CO_2$ conversion, as a function of the SEI, as predicted by the model. Electron

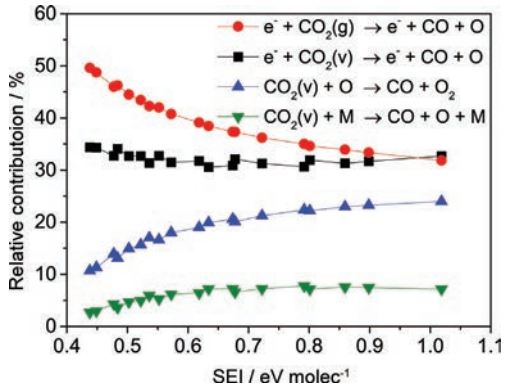


**Figure 6.** Calculated relative contributions of the various $CO_2$ dissociation processes to the overall $CO_2$ conversion, as a function of the SEI.

impact dissociation of $CO_2$, either from the ground state ($CO_{2(g)}$) or from the vibrational levels ($CO_{2(v)}$), appears to be the main dissociation mechanism. At the lowest SEI values investigated, electron impact dissociation from the $CO_2$ ground state contributes up to 50% to the $CO_2$ dissociation, but this value drops to 33% at the highest SEI values, whereas the contribution of electron impact dissociation from vibrationally excited $CO_2$ is about 30–35% at all SEI values investigated. The role of $CO_2$ dissociation upon collision of O atoms or any other molecule (indicated as M) with $CO_2$ molecules in vibrational levels slightly rises with SEI, and the relative contribution reaches about 24 and 7%, respectively, at the highest SEI values investigated. It is important to mention that electron impact dissociation from the $CO_2$ ground state is less energy efficient, as it requires more energy than strictly needed for dissociation (see below), whereas the dissociation processes from vibrationally excited $CO_2$ provides a more energy-efficient channel. The latter is especially true for the collisions of vibrationally excited $CO_2$ with O atoms, as the O atom formed upon dissociation of $CO_2$ in one of the other processes can be used to dissociate an extra $CO_2$ molecule. Figure 6 thus illustrates that $CO_2$ conversion in the GAP already proceeds in an energy efficient way, compared for instance to a DBD, in which electron impact dissociation from the ground state is the main mechanism;[15,21,68] however, that there is still room for improvement if we can further enhance the contributions of the processes involving vibrationally excited $CO_2$. More details on the calculated vibrational distribution function can be found in the Supporting Information.

The important role of the vibrational levels for energy-efficient $CO_2$ conversion in the GAP is in line with observations made for a classical gliding arc[69] and a MW plasma.[21,70,71] Indeed, the electron temperature in the GAP is about 1.68 eV, which is suitable for populating the lowest vibrational levels of $CO_2$. Subsequently, collisions between vibrationally excited $CO_2$ molecules, also called vibration–vibration relaxation, will gradually populate the higher vibrational levels, which will easily dissociate into CO and O atoms (either due to electron impact or upon collision with another O atom or any molecule; see Figure 6 above). This so-called ladder-climbing process is schematically illustrated in Figure 7. This process is very energy effi-

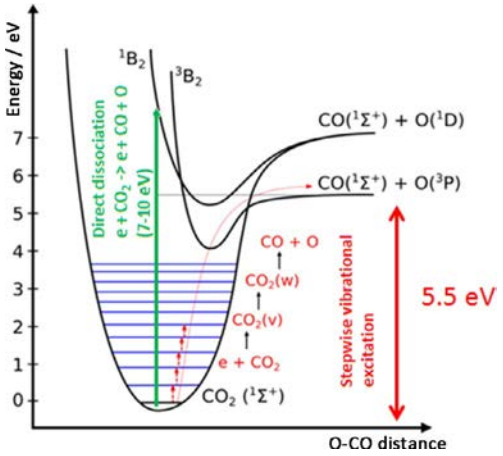


**Figure 7.** Schematic illustration of some $CO_2$ electronic and vibrational levels, illustrating the energy efficient dissociation process through stepwise vibrational excitation, that is, so-called ladder climbing, compared to direct dissociation through electronic excitation. Note that $CO_{2(v)}$ and $CO_{2(w)}$ stand for different vibrationally excited levels, with $CO_{2(w)}$ being a higher level than $CO_{2(v)}$.

cient, and thus it explains the good energy efficiency of the GAP, in contrast to, for instance, a DBD plasma, where the $CO_2$ conversion almost exclusively proceeds through electron impact electronic excitation from the ground state, as mentioned above. As seen from Figure 7, this process requires about 7–10 eV, which is more than the C=O bond energy of 5.5 eV. This extra energy can be considered as waste, and the latter explains why the energy efficiency of the DBD is lower than for the GAP (or MW plasma); see also next section.

The ladder climbing process, as well as the other processes illustrated in Figure 6 above, also explains why the energy cost of the GAP is lower, and the energy efficiency higher, compared to thermal dissociation. Indeed, in the GAP, the electrons heated by the applied power will selectively activate the $CO_2$ molecules, by vibrational excitation as well as electronic excitation, whereas the other degrees of freedom do not need to be activated, as is the case in thermal dissociation, in which the entire gas must be heated for the conversion to take place.

### Comparison of our results with other types of plasmas, as well as other novel $CO_2$ conversion technologies

To give an overview of where our results should be positioned in the rapidly expanding field of plasma-based $CO_2$ conversion, we plot in Figure 8 the energy efficiency of $CO_2$ splitting versus the conversion in different types of plasmas. The results are shown for all pressures, with open symbols indicating low pressure and solid symbols indicating atmospheric pressure or higher.

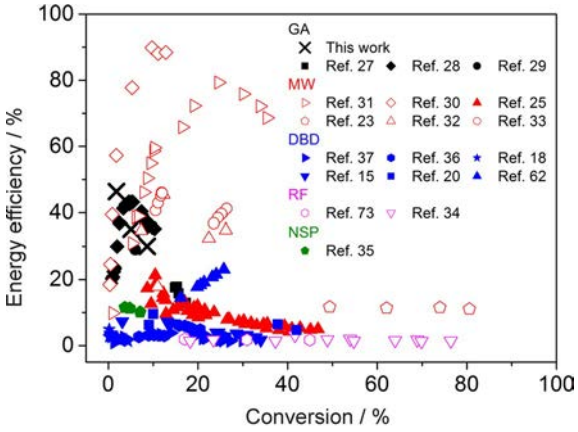


**Figure 8.** Energy efficiency versus conversion in different types of plasmas used for $CO_2$ conversion, and comparison with our data. The results are shown for all pressures, with open symbols indicating low pressure and solid symbols indicating atmospheric pressure or higher.

If we compare our data (indicated with black crosses) with the results of other experiments, we can conclude that in terms of energy efficiency, the GAP is very promising. Only Asisov et al.[30] and Rusanov et al.[31] obtained higher energy efficiency (i.e., up to 90 and 80%, respectively) with their MW plasma reactors. However, the discharge used by Asisov et al. was organized in a supersonic flow and the setup operated at a reduced pressure of 0.05–0.2 atm. Rusanov et al. also made use of a setup operating at reduced pressure (50–200 torr or 0.06–0.26 atm), and it was reported that the energy efficiency dramatically drops to values of about 5–20% when the pressure rises to 1 atm.[25,72] The excellent energy efficiencies obtained by Asisov et al. and Rusanov et al., back in 1981 and 1983, have not yet been reproduced since then. However, similar energy efficiencies as in our GAP were reached more recently with a MW reactor by van Rooij et al.[32] and Bongers et al.[33] They both obtained a higher conversion (i.e., up to 26%) than in our case, but again these experiments were conducted at reduced pressures of 200 mbar (0.2 atm) and 150–600 mbar (0.15–0.60 atm), respectively. If the pressure would be increased, the conversion and energy efficiency would again be lower, and the plasma would also be less stable. Moreover, the energy cost of the pumping system should also be accounted for, when operating at reduced pressure, and this would lower the overall energy efficiency.

As seen in Figure 8, both studies performed in radio-frequency (RF) plasma at low pressure show lower energy efficiency than in our GAP. This can be explained by the fact that the optimum operating conditions for vibrational excitation of $CO_2$, that is, having a specific energy input of $\approx 1$ eV molec$^{-1}$, an electron temperature of $\approx 1$ eV and an ionization degree ($n_e/n_0$) $\geq 10^{-6}$ are not met in this type of plasma.[34,73]

Because operation at atmospheric pressure is generally more compatible with industrial applications, it is better to compare with results obtained at 1 atm (or higher), as plotted with solid symbols in Figure 8. In a MW plasma, the energy efficiency is then typically lower, that is, in the range of 5–20%.[25] In this specific case, the conversion is higher than in our GAP. However, these experiments were conducted at a higher power (up to 2 kW).

We also plot in Figure 8 the results obtained in a DBD, which is very often used for $CO_2$ conversion. It is clear that the energy efficiency of the studies conducted with DBD[15,18,20,36,37,62] are much lower than our results. This is again due to the non-ideal operating conditions, as the SEI and electron temperature are typically higher than 1 eV molec$^{-1}$ and 1 eV, respectively. Therefore, the energy-efficient vibrational excitation is not favored.

The energy efficiency obtained with NSP by Bak et al.[35] is also lower than in our case, at slightly lower conversion values. In this configuration, the pressure reached values from 2.4 to 5.1 atm. This can explain the lower energy efficiency. Moreover, in this type of plasma the average electron energy is rather high. Therefore, the excitation and auto-dissociation of $CO_2$ (10.5 eV) is the dominant reaction path instead of the vibrational excitation–dissociation pathway, which is more efficient.

Finally, if we compare our results with data obtained in other gliding arc plasmas, we can distinguish two groups, that is, on one hand the results obtained by Nunnally et al.[28] and Liu et al.,[29] which are similar to our results, and on the other hand the data of Indarto et al.[27] The difference between these two groups is the flow configuration that was used. Nunnally et al. and Liu et al. used a vortex flow, like in our case, whereas the results of Indarto et al.[27] were obtained in a classical gliding arc configuration. This comparison clearly shows that a vortex flow increases the energy efficiency of $CO_2$ conversion, because it stabilizes the plasma in the middle of the reactor and the gas flow is forced to go through the plasma, whereas the heat lost to the reactor walls is minimized.

In general, we can conclude that the energy efficiency is typically much higher in a gliding arc discharge as well as in MW plasmas than in the other plasma types. This can be explained by the fact that the electron energy is in the order of 1 eV in gliding arc and MW discharges, and therefore vibrational excitation of the $CO_2$ molecules is favored, whereas the electron energy in other plasma types such as DBD, RF, and NSP is typically somewhat higher, yielding mainly electronic excitation of $CO_2$, leading to a waste of energy, as explained in the previous section. To summarize, we can conclude from Figure 8 that the GAP performs better at atmospheric pressure than all the other plasma types.

Plasma technology is obviously not the only technology of interest for $CO_2$ conversion. Therefore, it is necessary to compare our plasma process with other alternatives for the production of fuels from sunlight. One of the primary indicators used to compare different technologies is the solar-to-fuel energy conversion efficiency ($\eta_{solar\text{-}to\text{-}fuel}$). This is a measure of how well solar energy is converted to chemical energy of the fuel. If we assume that the electricity needed for our plasma process is produced by solar panels, which have an efficiency of 25%, we currently can reach a solar-to-fuel efficiency of 11.5%. We are aware that CO is not a mainstream fuel. However, it has a heating value and can therefore be used to define a solar-to-fuel efficiency in a correct manner. The splitting of $CO_2$ by means of plasma can be seen as an efficient source of CO, to produce fuels in combination with $H_2$. On the other hand, when $CO_2$ is mixed with a hydrogen source in the plasma, syngas and other (liquid) fuels can be produced directly. Moreover, if we add a catalyst to the system to improve the selectivity, synergies due to plasma and catalyst may arise, as explained in [74]. This opens up an array of interesting investigative routes, which we will look into in the future.

A competitive technology that also uses electricity for the production of fuels is water electrolysis. For photovoltaics (PV) powered water electrolysis, $\eta_{solar\text{-}to\text{-}fuel} = 7\text{–}10\%$.[75] Other novel conversion technologies, like photocatalytic and solar thermochemical conversion, use direct sunlight to produce fuels. Theoretically, the solar-to-fuel efficiency of photocatalytic conversion is limited to a maximum of 17% owing to the band gap energy of the photocatalyst.[76] However, the solar energy-conversion efficiencies obtained to date are much lower ($<2\%$).[75] For the solar thermochemical approach, theoretical $\eta_{solar\text{-}to\text{-}fuel}$ values exceeding 30% are often assumed, but solar-to-fuel energy conversion efficiencies above 10% are still pending experimental demonstration with robust and scalable solar reactors.[8,11,75] A value of 20% is likely needed for solar fuels to be cost competitive.[77]

From these comparisons it becomes evident that our results currently obtained are less than a factor of two away from being cost competitive and already outperform several other novel technologies. Moreover, both our experiments and simulations indicate that there is still room for improvement of the GAP and we can reach even higher values in the future. Also, the overall energy efficiency can be improved when the efficiency of solar panels can be further enhanced or by producing the electricity needed for the plasma process with another renewable energy source. The latter option is not possible for photochemical and solar thermochemical technologies since their primary source of energy originates from sunlight.

## Conclusions

In this work, we have investigated the performance of a novel type of gliding arc, the gliding arc plasmatron (GAP), for the conversion of $CO_2$, and evaluated it depending on its energy cost and efficiency for a wide range of conditions of plasma power and gas flow rate, and for different anode diameters of the setup. The best performance, in terms of both conversion and energy cost/efficiency, was reached in the configuration with the smallest anode diameter of 7.08 mm. The highest conversion of 8.6% was obtained at an energy cost of 39 kJ L$^{-1}$ (or 9.7 eV molec$^{-1}$) and an energy efficiency of 30%, whereas the highest energy efficiency in this configuration was 35%, corresponding to an energy cost of 33 kJ L$^{-1}$ (or 8.3 eV molec$^{-1}$), but at a somewhat reduced conversion of 5.1%. The reason that the configuration with the smallest anode diameter yields the best results can be understood from our gas-flow calculations, which demonstrate that the reverse vortex flow (RVF) is most strongly pronounced in this case. This RVF is indeed important for obtaining the highest $CO_2$ conversion, because it stabilizes the plasma in the middle of the reactor, as supported by our 3D plasma simulations, and the gas flow is forced to go through the plasma, while the heat lost to the reactor walls is minimized. The highest energy efficiency of 46% is reached with the GAP at an energy cost of 25 kJ L$^{-1}$ (or 6.3 eV molec$^{-1}$) and a corresponding conversion of 1.8%.

In general, we can conclude that the GAP is very promising for $CO_2$ conversion and we believe there is still room for improvement. We compared our results with the conversion and energy efficiency of thermal $CO_2$ splitting, as well as with results of other types of plasmas and novel $CO_2$ conversion technologies. It is very striking that the conversion and energy efficiency are much higher in the GAP compared to thermal $CO_2$ conversion, owing to the non-equilibrium properties of the plasma, as the chemistry of the conversion process is induced by energetic electrons. Also when compared to other types of plasmas, it is clear that the GAP is the most promising candidate for $CO_2$ conversion, as this type of discharge operates at atmospheric pressure and produces electrons with a typical energy in the order of 1 eV, which can vibrationally excite the $CO_2$ molecules, so that they can split into CO and $O_2$ in an energy efficient way through the ladder-climbing process. Furthermore, from the comparison with other novel $CO_2$ conversion technologies it becomes evident that our results here reported are less than a factor of two away from being cost competitive and already outperform several other novel technologies.

Our results indicate that the conversion rises upon lowering the flow rate because of the longer gas residence time in the reactor. However, the flow rate is limited in the current reactor setup, because a minimum flow rate is necessary to obtain a good vortex flow. Another way to increase the residence time in the reactor would be to increase the length of the cathode. We believe that this might further enhance the conversion, if a suitable vortex flow pattern can still be realized. This option will be investigated in future research.

Finally, we supported our experimental data with model calculations for the plasma chemistry, and obtained excellent agreement for the $CO_2$ conversion, energy cost, and energy efficiency. This indicates that we can use the model to elucidate the underlying plasma chemical processes of $CO_2$ conversion in the GAP. It is clear that vibrationally excited $CO_2$ significantly contributes to the $CO_2$ dissociation, and this can explain the good energy efficiency of $CO_2$ conversion. Furthermore, our simulations indicate that there is still room for improvement

by exploiting even more the non-equilibrium character of the GAP, for example, by operating at conditions in which the temperature inside the arc can be reduced, so that the vibrational distribution function of $CO_2$ becomes more non-thermal.

## Experimental Section

### Description of the experiments

#### *Gliding arc setup*

The experiments were performed with a GAP, as developed by Nunnally et al.[28] This is a three-dimensional gliding arc reactor in which the gas flow enters through a tangential inlet so that a vortex flow is obtained (see Figure 9). A potential difference is applied between the cathode and anode, creating an arc discharge. Depending on the electrode configuration, more specifically the diameter of the reactor body (acting as cathode) and the outlet of the reactor (acting as anode), two vortex flow patterns can be obtained: forward vortex flow (FVF) or reverse vortex flow (RVF). When the anode diameter is equal to the cathode diameter, the gas flow enters and follows a spiral trajectory both toward the bottom and the top of the reactor. The reactor outlet is found at the bottom of the reactor, so the gas will leave the reactor in a so-called FVF. On the other hand, when the anode diameter is smaller than the cathode diameter, the incoming gas cannot immediately exit the reactor, and it will first be forced upwards in the cathodic part of the reactor. Due to friction and inertia it loses rotational speed, so when arriving at the top of the reactor, it will start to move in a vortex towards the bottom, that is, reverse direction, but in a smaller vortex, so that it can now exit the reactor at the bottom. The arc plasma is stabilized in the center of the reactor by this vortex flow and the reverse vortex gas flow is actually forced to go through the plasma (see Figure 9). Figure 10 presents a photograph of the gliding arc plasma, illustrating that it is stabilized in the center of the reactor and clearly showing where the arc is attached to the electrodes.

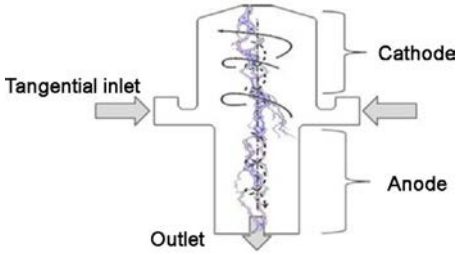


**Figure 9.** Schematic picture of the gliding arc plasmatron in reverse vortex flow configuration. Both the forward and reverse vortex flows are indicated (with full and dashed spirals, respectively). This vortex flow configuration stabilizes the arc discharge (indicated in purple) in the center of the reactor and forces the reverse gas flow to go through the plasma.

To compare the performance of the RVF and FVF configurations, we used four different stainless steel electrodes, that is, a high voltage electrode and three grounded electrodes. The high voltage electrode, which acts as the cathode (see Figure 9), has a length of 20.30 mm and a diameter of 17.50 mm. All grounded electrodes, acting as anode, have the same length (16.30 mm) but their diameter is 7.08, 14.20, and 17.50 mm, respectively. These dimensions

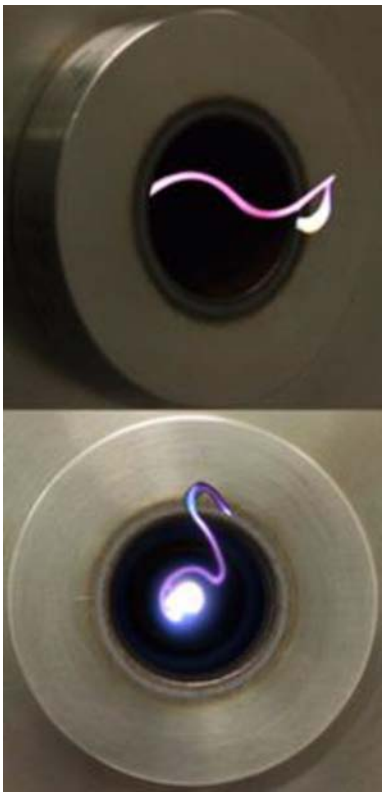

**Figure 10.** Photos of the outlet of the GAP (anode), showing the arc discharge. The arc is stabilized in the middle of the reactor, where it is attached to the cathode and anode.

gave rise to a reactor volume of 6.22, 6.93, and 7.43 $cm^3$, respectively, but the arc volume was only about 0.13 $cm^3$. A photograph and diagram of the entire experimental system is shown in Figure 11.

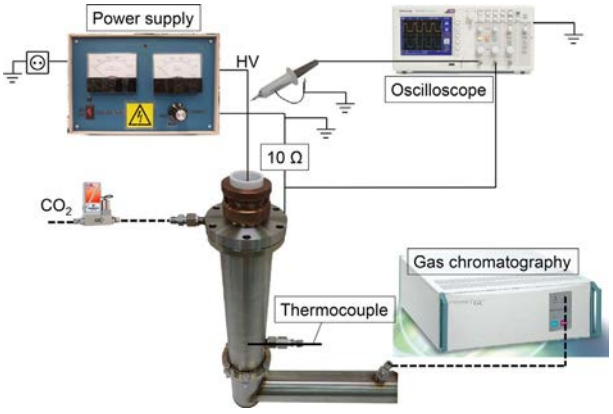


**Figure 11.** Schematics of the entire experimental system.

A mass-flow controller (Bronkhorst) was used to insert $CO_2$ into the GAP. The $CO_2$ flow rate was varied between 10 and 22 $L_n min^{-1}$. $CO_2$ with a purity of 99.5% was used and no preheating of the gas occurred. The reactor was powered by a DC current source type power supply. The plasma voltage and current were measured by a high-voltage probe (Tektronix P6015A) and a current sense resistor of 10 Ω, respectively. The electrical signals were sampled by

a two-channel digital storage oscilloscope (Tektronix TDS2012C). The current was varied between 0.04 and 0.38 A. The plasma power is calculated as follows:

$$P_{plasma} = 1/T \int_0^{t=T} V_{plasma} \times I_{plasma} dt \quad (1)$$

where $P$ is the power in watts, $T$ is the period, $V$ is the voltage in volts, and $I$ is the current in amps. In the reactor tube, which is placed after the GAP, a thermocouple is inserted to measure the temperature of the effluent stream. The output gas composition is analyzed online by gas chromatography.

### Gas analysis

The feed and product gases were analyzed by a three-channel compact gas chromatograph (CGC) from Interscience. This device has three different ovens, each with their own column and detector. A Molsieve 5A and Rt-Q-Bond column were used to separate $O_2$ and CO, which were detected with a thermal conductivity detector (TCD). The other channel was equipped with a Rt-Q-Bond column and TCD for the measurement of $CO_2$.

The conversion of $CO_2$, $X_{CO_2}$, is defined as:

$$X_{CO_2}[\%] = \frac{\dot{n}_{CO_{2(in)}} - \dot{n}_{CO_{2(out)}}}{\dot{n}_{CO_{2(in)}}} \times 100\% \quad (2)$$

where $\dot{n}_{CO_{2(in)}}$ and $\dot{n}_{CO_{2(out)}}$ are the molar flow rate of $CO_2$ without and with plasma, respectively. As the method mentioned above does not account for the gas expansion due to $CO_2$ splitting, a correction factor is used, which is explained in the Supporting Information.[61]

To calculate the energy efficiency of $CO_2$ conversion, the SEI in the plasma is defined as:

$$SEI\ [kJ\ L^{-1}] = \frac{\text{Plasma power [kW]}}{\text{Flow rate } [L_n\ min^{-1}]} \times 60\ s\ min^{-1} \quad (3)$$

where the flow rate is expressed in $L_n min^{-1}$ (liters normal per minute) with reference conditions at a temperature of 0 °C and a pressure of 1 atm.

The energy cost (EC) for converting $CO_2$ is calculated as follows:

$$EC_{CO_2}[kJ\ L^{-1}] = \frac{SEI\ [kJ\ L^{-1}]}{X_{CO_2}} \quad (4)$$

Likewise, the energy efficiency, $\eta$, is calculated as:

$$\eta\ [\%] = \frac{\Delta H_R\ [kJ\ mol^{-1}] \times X_{CO_2}[\%]}{SEI\ [kJ\ L^{-1}] \times 22.4\ L\ mol^{-1}} \quad (5)$$

where $\Delta H_R$ is the reaction enthalpy of $CO_2$ splitting (i.e., 279.8 kJ mol$^{-1}$), $X_{CO_2}$ is the amount of $CO_2$ converted, SEI is defined above and 22.4 L mol$^{-1}$ is the molar volume at 0 °C and 1 atm.

Every experiment was performed three times. Subsequently, a propagation of uncertainty was applied to the results to calculate the error bars.

### Description of the modeling work

To understand the effect of the different electrode configurations, we calculated the 3D gas flow pattern in the different reactor setups, with COMSOL Multiphysics Simulation Software, based on solving the Navier–Stokes equations, assuming a turbulent flow. The details are explained in the Supporting Information.

To describe the plasma chemistry of $CO_2$ conversion in the GAP, and to elucidate the underlying mechanisms, we developed a 0D plasma chemistry model, which allows to describe the behavior of a large number of species, and incorporate a large number of chemical reactions, with limited computational effort. In this 0D chemical kinetics model, called ZDPlaskin, balance equations were used to calculate the time-evolution of the species densities, taking into account the various production and loss terms by chemical reactions. From these species densities the $CO_2$ conversion can be obtained, and in combination with the plasma power and gas flow rate (and thus the SEI), this also yields the energy cost and energy efficiency, in the same way as explained above [see Equations (4) and (5)]. Besides that, the model also calculates the gas temperature, the electron density, and electron temperature. The model is described in more detail in the Supporting Information.

## Acknowledgements

*We acknowledge financial support from the IAP/7 (Inter-university Attraction Pole) program "PSI-Physical Chemistry of Plasma-Surface Interactions" by the Belgian Federal Office for Science Policy (BELSPO), the Fund for Scientific Research Flanders (FWO; Grant no. G.0383.16 N and 11U5316N) and the European Marie Skłodowska-Curie Individual Fellowship "GlidArc" within Horizon2020 (Grant No. 657304). The calculations were done using the Turing HPC infrastructure at the CalcUA core facility of the Universiteit Antwerpen (UAntwerpen), a division of the Flemish Supercomputer Center VSC, funded by the Hercules Foundation, the Flemish Government (department EWI) and the UAntwerpen. Finally, we also want to thank A. Rabinovich, A.P.J van Deursen, T. Huiskamp and J. Liu for the very interesting discussions.*

## *Conflict of interest*

*The authors declare no conflict of interest.*

**Keywords:** co$_2$ conversion · energy efficiency · gliding arc plasmatron · plasma modeling · vortex flow

[1] a) L. Johnson, J. Grant, P. L. Low, *Two Degrees of Separation: Ambition and Reality: Low Carbon Economy Index 2014*, **2014** https://www.pwc.co.uk/assets/pdf/low-carbon-economy-index-2014.pdf, b) C. B. Field et al., *IPCC, 2014: Climate Change 2014 Impacts, Adaptation, and Vulnerability Part A: Global and Sectoral Aspects. Contribution of Working Group II, to the Fifth Asessment Report of the Intergovernmental Panel on Climate Change*, **2014** https://environmentalmigration.iom.int/climate-change-2014-impacts-adaptation-and-vulnerability-contribution-working-group-ii-fifth.

[2] Daily $CO_2$ values: https://www.co2.earth/daily-co2, accessed on March 2017.

[3] G. Centi, S. Perathoner, *Catal. Today* **2009**, *148*, 191 – 205.

[4] G. Centi, E. A. Quadrelli, S. Perathoner, *Energy Environ. Sci.* **2013**, *6*, 1711 – 1731.
[5] W. McDonough, M. Braungart, P. Anastas, J. Zimmerman, *Environ. Sci. Technol.* **2003**, *37*, 434A – 441A.
[6] E. E. Benson, C. P. Kubiak, A. J. Sathrum, J. M. Smieja, *Chem. Soc. Rev.* **2009**, *38*, 89 – 99.
[7] M. Aresta, A. Dibenedetto, A. Angelini, *Chem. Rev.* **2014**, *114*, 1709 – 1742.
[8] J. R. Scheffe, A. Steinfeld, *Mater. Today* **2014**, *17*, 341 – 348.
[9] E. V. Kondratenko, G. Mul, J. Baltrusaitis, G. O. Larrazabal, J. Perez-Ramirez, G. O. Larrazábal, J. Pérez-Ramírez, *Energy Environ. Sci.* **2013**, *6*, 3112.
[10] A. Goeppert, M. Czaun, J.-P. Jones, G. K. Surya Prakash, G. A. Olah, *Chem. Soc. Rev.* **2014**, *43*, 7995 – 8048.
[11] A. H. McDaniel, E. C. Miller, D. Arifin, A. Ambrosini, E. N. Coker, R. O'Hayre, W. C. Chueh, J. Tong, *Energy Environ. Sci.* **2013**, *6*, 2424.
[12] E. N. Coker, A. Ambrosini, M. a. Rodriguez, J. E. Miller, *J. Mater. Chem.* **2011**, *21*, 10767.
[13] S. Samukawa, M. Hori, S. Rauf, K. Tachibana, P. Bruggeman, G. Kroesen, J. C. Whitehead, A. B. Murphy, A. F. Gutsol, S. Starikovskaia, U. Kortshagen, J.-P- Boeuf, T. J. Sommerer, M. J. Kushner, U. Czarnetzki, N. Mason, *J. Phys. D* **2012**, *45*, 253001.
[14] A. Bogaerts, E. Neyts, R. Gijbels, J. van der Mullen, *Spectrochim. Acta Part B* **2002**, *57*, 609 – 658.
[15] R. Aerts, W. Somers, A. Bogaerts, *ChemSusChem* **2015**, *8*, 702 – 716.
[16] M. Ramakers, I. Michielsen, R. Aerts, V. Meynen, A. Bogaerts, *Plasma Processes Polym.* **2015**, *12*, 755 – 763.
[17] R. Aerts, T. Martens, A. Bogaerts, *J. Phys. Chem. C* **2012**, *116*, 23257 – 23273.
[18] F. Brehmer, S. Welzel, M. C. M. Van De Sanden, R. Engeln, *J. Appl. Phys.* **2014**, *116*, 123303.
[19] R. Aerts, R. Snoeckx, A. Bogaerts, *Plasma Processes Polym.* **2014**, *11*, 985 – 992.
[20] K. Van Laer, A. Bogaerts, *Energy Technol.* **2015**, *3*, 1038 – 1044.
[21] T. Kozák, A. Bogaerts, *Plasma Sources Sci. Technol.* **2014**, *23*, 045004.
[22] A. P. H. Goede, W. Bongers, M. G. Graswinckel, R. M. C. Van De Sanden, M. Leins, J. Kopecki, A. Schulz, M. Walker, *EPJ Web Conf.* **2014**, *79*, 01005.
[23] T. Silva, N. Britun, T. Godfroid, R. Snyders, *Plasma Sources Sci. Technol.* **2014**, *23*, 025009.
[24] S. Heijkers, R. Snoeckx, T. Kozák, T. Silva, T. Godfroid, N. Britun, R. Snyders, A. Bogaerts, *J. Phys. Chem. C* **2015**, *119*, 12815 – 12828.
[25] L. F. Spencer, A. D. Gallimore, *Plasma Sources Sci. Technol.* **2013**, *22*, 015019.
[26] A. Indarto, J. Choi, H. Lee, H. K. Song, *Environ. Eng. Sci.* **2006**, *23*, 1033 – 1043.
[27] A. Indarto, D. R. Yang, J. W. Choi, H. Lee, H. K. Song, *J. Hazard. Mater.* **2007**, *146*, 309 – 315.
[28] T. Nunnally, K. Gutsol, A. Rabinovich, A. Fridman, A. Gutsol, A. Kemoun, *J. Phys. D* **2011**, *44*, 274009.
[29] J. L. Liu, H. W. Park, W. J. Chung, D. W. Park, *Plasma Chem. Plasma Process.* **2015**, https://doi.org/10.1007/s11090-015-9649-9642.
[30] R. I. Asisov, A. K. Vakar, V. K. Jivotov, M. F. Krotov, O. A. Zinoviev, B. V. Potapkin, A. A. Rusanov, V. D. Rusanov, A. A. Fridman, *Proc. USSR Acad. Sci.* **1983**, *271*, .
[31] V. D. Rusanov, A. Fridman, G. V. Sholin, *Sov. Phys. Usp.* **1981**, *24*, 447 – 474.
[32] G. J. van Rooij, D. C. M. van den Bekerom, N. den Harder, T. Minea, G. Berden, W. A. Bongers, R. Engeln, M. F. Graswinckel, E. Zoethout, M. C. M. van de Sanden, *Faraday Discuss.* **2015**, *183*, 233 – 248.
[33] W. Bongers, H. Bouwmeester, B. Wolf, F. Peeters, S. Welzel, D. van den Bekerom, N. den Harder, A. Goede, M. Graswinckel, P. W. Groen, et al., *Plasma Process. Polym.* **2016**, https://doi.org/10.1002/ppap.201600126.
[34] L. F. Spencer, A. D. Gallimore, *Plasma Chem. Plasma Process.* **2011**, *31*, 79 – 89.
[35] M. S. Bak, S. K. Im, M. Cappelli, *IEEE Trans. Plasma Sci.* **2015**, *43*, 1002 – 1007.
[36] Q. Yu, M. Kong, T. Liu, J. Fei, X. Zheng, *Plasma Chem. Plasma Process.* **2012**, *32*, 153 – 163.
[37] S. Paulussen, B. Verheyde, X. Tu, C. De Bie, T. Martens, D. Petrovic, A. Bogaerts, B. Sels, *Plasma Sources Sci. Technol.* **2010**, *19*, 034015.
[38] X. Tao, M. Bai, X. Li, H. Long, S. Shang, Y. Yin, X. Dai, *Prog. Energy Combust. Sci.* **2011**, *37*, 113 – 124.
[39] G. Petitpas, J. D. Rollier, A. Darmon, J. Gonzalez-Aguilar, R. Metkemeijer, L. Fulcheri, *Int. J. Hydrogen Energy* **2007**, *32*, 2848 – 2867.
[40] C. J. Liu, G. H. Xu, T. Wang, *Fuel Process. Technol.* **1999**, *58*, 119 – 134.
[41] R. Snoeckx, Y. X. Zeng, X. Tu, A. Bogaerts, *RSC Adv.* **2015**, *5*, 29799 – 29808.
[42] A. Janeco, N. R. Pinhão, V. Guerra, *J. Phys. Chem. C* **2015**, *119*, 109 – 120.
[43] R. Snoeckx, R. Aerts, X. Tu, A. Bogaerts, *J. Phys. Chem. C* **2013**, *117*, 4957 – 4970.
[44] G. Scarduelli, G. Guella, D. Ascenzi, P. Tosi, *Plasma Processes Polym.* **2011**, *8*, 25 – 31.
[45] Y. P. Zhang, Y. Li, Y. Wang, C. J. Liu, B. Eliasson, *Fuel Process. Technol.* **2003**, *83*, 101 – 109.
[46] X. Zhang, M. S. Cha, *J. Phys. D* **2013**, *46*, 415205.
[47] L. M. Martini, G. Dilecce, G. Guella, A. Maranzana, G. Tonachini, P. Tosi, *Chem. Phys. Lett.* **2014**, *593*, 55 – 60.
[48] D. Li, X. Li, M. Bai, X. Tao, S. Shang, X. Dai, Y. Yin, *Int. J. Hydrogen Energy* **2009**, *34*, 308 – 313.
[49] X. Tu, H. J. Gallon, M. V. Twigg, P. A. Gorry, J. C. Whitehead, *J. Phys. D* **2011**, *44*, 274007.
[50] B. Eliasson, C. Liu, U. Kogelschatz, *Ind. Eng. Chem. Res.* **2000**, *39*, 1221 – 1227.
[51] V. J. Rico, J. L. Hueso, J. Cotrino, A. R. González-Elipe, *J. Phys. Chem. A* **2010**, *114*, 4009 – 4016.
[52] X. Tu, J. C. Whitehead, *Appl. Catal. B* **2012**, *125*, 439 – 448.
[53] Q. Wang, Y. Cheng, Y. Jin, *Catal. Today* **2009**, *148*, 275 – 282.
[54] B. Fidalgo, A. Domínguez, J. J. Pis, J. A. Menéndez, *Int. J. Hydrogen Energy* **2008**, *33*, 4337 – 4344.
[55] A. Indarto, J. W. Choi, H. Lee, H. K. Song, *Energy* **2006**, *31*, 2986 – 2995.
[56] B. Eliasson, U. Kogelschatz, B. Xue, L.-M. Zhou, *Ind. Eng. Chem. Res.* **1998**, *37*, 3350 – 3357.
[57] M. Kano, G. Satoh, S. Iizuka, *Plasma Chem. Plasma Process.* **2012**, *32*, 177 – 185.
[58] T. Ihara, M. Kiboku, Y. Iriyama, *Bull. Chem. Soc. Jpn.* **1994**, *67*, 312 – 314.
[59] T. Ihara, T. Ouro, T. Ochiai, M. Kiboku, Y. Iriyama, *Bull. Chem. Soc. Jpn.* **1996**, *69*, 241 – 244.
[60] G. Chen, T. Silva, V. Georgieva, T. Godfroid, N. Britun, R. Snyders, M. P. Delplancke-Ogletree, *Int. J. Hydrogen Energy* **2015**, *40*, 3789 – 3796.
[61] R. Snoeckx, S. Heijkers, K. Van Wesenbeeck, S. Lenaerts, A. Bogaerts, *Energy Environ. Sci.* **2016**, *9*, 999 – 1011.
[62] A. Ozkan, T. Dufour, T. Silva, N. Britun, R. Snyders, F. Reniers, A. Bogaerts, *Plasma Sources Sci. Technol.* **2016**, *25*, 055005.
[63] M. Scapinello, L. M. Martini, G. Dilecce, P. Tosi, *J. Phys. D* **2016**, *49*, 075602.
[64] X. S. Li, B. Zhu, C. Shi, Y. Xu, A. M. Zhu, *AIChE J.* **2011**, *57*, 2854.
[65] B. Zhu, X. S. Li, C. Shi, J. L. Liu, T. L. Zhao, A. M. Zhu, *Int. J. Hydrogen Energy* **2012**, *37*, 4945.
[66] B. Zhu, X. S. Li, J. L. Liu, X. Zhu, A. M. Zhu, *Chem. Eng. J.* **2015**, *264*, 445.
[67] A. Gutsol, A. Rabinovich, A. Fridman, *J. Phys. D* **2011**, *44*, 274001.
[68] A. Bogaerts, T. Kozák, K. van Laer, R. Snoeckx, *Faraday Discuss.* **2015**, *183*, 217 – 232.
[69] W. Wang, A. Berthelot, S. Kolev, X. Tu, A. Bogaerts, *Plasma Sources Sci. Technol.* **2016**, *25*, 065012.
[70] T. Kozák, A. Bogaerts, *Plasma Sources Sci. Technol.* **2015**, *24*, 015024.
[71] A. Berthelot, A. Bogaerts, *Plasma Sources Sci. Technol.* **2016**, *25*, 045022.
[72] A. Fridman, *Plasma Chemistry*, Cambridge University Press, New York, **2008**.
[73] S. Y. Savinov, H. Lee, H. K. Song, B.-K. Na, *Korean J. Chem. Eng.* **2002**, *19*, 564 – 566.
[74] E. C. Neyts, K. Ostrikov, M. K. Sunkara, A. Bogaerts, *Chem. Rev.* **2015**, *115*, 13408 – 13446.
[75] G. P. Smestad, A. Steinfeld, *Ind. Eng. Chem. Res.* **2012**, *51*, 11828 – 11840.
[76] S. C. Roy, O. K. Varghese, M. Paulose, C. A. Grimes, *ACS Nano* **2010**, *4*, 1259 – 1278.
[77] P. Furler, J. R. Scheffe, A. Steinfeld, *Energy Environ. Sci.* **2012**, *5*, 6098 – 6103.

Manuscript received: April 7, 2017
Accepted manuscript online: May 8, 2017
Version of record online: May 22, 2017